

Optimization of chirped and tapered microstrip Koch Fractal Electromagnetic Band Gap (KFEBG) structures for improved low-pass filter design

Juan de Dios Ruiz, Félix L. Martínez-Viviente and Juan Hinojosa

Departamento de Electrónica, Tecnología de Computadoras y Proyectos, Universidad Politécnica de Cartagena, Plaza del Hospital 1, 30202 Cartagena, Spain

E-mail: felix.martinez@upct.es

Abstract: This manuscript presents electromagnetic bandgap (EBG) structures in microstrip technology based on one-dimensional (1-D) Koch fractal patterns (KFEBG). This fractal geometry allows to adjust the radius r and distance a between patterns so that a low-pass filter response is obtained when the ratio r/a is higher than 0.5. However, in such case undesired strong ripples appear in the low bandpass region. We demonstrate that the performance in the passband of this filter can be improved by applying a tapering function to the Koch fractal dimensions and to the width of the microstrip line, while simultaneously chirping (modulating) the Koch fractal periodic pattern distance (a) so as to maintain a constant r/a ratio. Several tapering functions scaled by a factor K are presented, and the results of their application to the KFEBG microstrip structure are compared by means of relevant characteristic parameters. Optimal performance has been obtained for the Kaiser and Cauchy distributions applied to the Koch fractal pattern, combined with a rectangular and Cauchy distribution applied to the microstrip width, respectively.

1 INTRODUCTION

Electromagnetic band gap structures (EBG) in microstrip technology were first proposed at the end of the past century [1-2]. An EBG structure consists on a periodic structure that exhibits a band of frequencies in which the electromagnetic propagation is not allowed. Therefore EBG structures can be used as Bragg reflectors. In microstrip technology, structures with a periodic pattern etched in the ground plane have been proposed as the most simple and effective Bragg reflectors [2-4]. Circular [2-3], sinusoidal and triangular [4] shapes are typically etched as periodic patterns.

In fractal EBG devices, fractal shapes are etched as periodic patterns in the ground plane [5-8]. When the fractal pattern is based on the Koch curve, the EBG structure is named Koch fractal electromagnetic band gap (KFEBG). KFEBGs have the remarkable advantage that they allow the realization of structures with r/a (radii/period) ratios higher than 0.5. This has the important consequence that Bragg reflectors become low-pass filters [7-8]. However, their behavior in the passband is not optimal, because they present a significant amount of ripple. Tapering techniques can be employed to improve performance in the low-passband, so that the filter characteristics in this frequency range can be comparable to Bragg reflectors with r/a lower than 0.5 [9-10]. We have explained the design of KFEBG filters in a previous paper [7].

The aim of this manuscript is to apply tapering techniques to the radii of periodic fractals etched in the ground plane of KFEBG structures according to several mathematical distributions, together with a corresponding chirping of the period a of the structure in order to maintain a constant r/a ratio. Similar tapering functions will be applied to the microstrip line width scaled by a factor K . The influence of this K factor in the optimization of the results is presented in this paper. By combining the application of different tapering distributions to the sizes of the fractals in the ground plane with various distribution functions to the

microstrip width, we obtain an optimal response in the low pass region evaluated according to the following parameters: size reduction, ripple level, return loss, medium value of S_{11} in the passband, and band width of the bandpass filter.

As a conclusion of this work we will show simulated and measured performance of optimal structures with r/a ratio equal to 0.5. This value has been demonstrated to be the limit between low pass filter and Bragg reflector behavior in EBG structures [7], and represents a compromise between performance in the bandpass (ripple reduction) and high frequency rejection.

2 TAPERING FUNCTION

Tapering functions have been widely used to improve the performance of conventional EBG [9-11] and non-conventional EBG structures [8], as well as other devices such as free electron maser Bragg resonators composed of periodic cylindrically symmetric corrugations [12] and optical fiber Bragg gratings [13]. Originally, tapering functions were employed in digital filters as sampling windows [14].

In our application, the tapering function on the ground plane modifies the periodic fractal pattern shown in Fig. 1a, so that the fractal radius distribution is given by the equation:

$$r_i = r_{\max} \cdot T(z_i/L) \quad i = 0, 1, \dots \quad (1)$$

where r_i and r_{\max} are the i -th and maximum Koch fractal hexagonal cell radii, respectively, (z_i/L) is the normalized longitudinal position in the circuit ($z_0=0$ corresponds to the central point), and $T(z_i/L)$ is the tapering distribution. In a previous work [8] we have already shown the effects of applying a tapering window to the fractal pattern etched in the KFEBG ground plane, which takes the form shown in Fig. 1b.

When the tapering distribution is applied to conventional EBG and KFEBG structures, the frequency response is improved as a consequence of the progressive matching that the

tapering function produces between the characteristic impedance of the Bloch wave and the input and output characteristic impedance of the waveguide, [8], [10],[15-17].

Four distribution functions have been studied for this work, as shown in Fig. 2: Cauchy [14], Kaiser [8-10], Gauss [9-10], and rectangular or uniform function [14], in order from sharpest to less pronounced shape.

The Cauchy distribution is given by the following equation:

$$T(z/L) = \frac{1}{1 + \left(5 \frac{z}{L}\right)^2} \quad (2)$$

On the other hand, the Kaiser distribution is given in terms of Bessel functions according to the following equation:

$$T(z/L) = \frac{I_0\left(4\sqrt{1 - (2z/L)^2}\right)}{I_0(4)}, \quad (3)$$

where I_0 is the first-class modified Bessel function. Finally, the Gauss distribution function is:

$$T(z/L) = e^{-\left(\frac{z}{L}\right)^2} \quad (4)$$

and the uniform or rectangular function is given by:

$$T(z/L) = \begin{cases} 1 & \text{if } -0.4 \leq (z/L) \leq 0.4 \\ 0 & \text{otherwise} \end{cases} \quad (5)$$

The tapering of the radii of the Koch fractals according to the previous distributions has as a consequence a decrease of the ratio r/a as we move from the center to the edges of the structure. Since the low pass behavior of the filter is an effect of the r/a ratio being above the 0.5 upper limit of conventional non-fractal EBG structures that behave as Bragg reflectors, the decrease of this ratio below such limit degrades the rejection of high frequencies. In order to compensate this effect, and at the same time to obtain a more compact

size of the device, we have taking the following approach [8]. Instead of using a fixed period a , we modify it in proportion to the radii of the Koch fractal cells so that the distance a_i between the centers of adjacent Koch fractal hexagonal cells follows a linear proportion:

$$a_i = r_{i-1}/C \quad i = 1, 2, \dots \quad (6)$$

where r_0 corresponds to r_{max} , r_{i-1} is the radii of the Koch fractal tapered cells, and C is a constant equal to the initial r/a ratio value of the non-tapered KFEBG microstrip structure as shown in Fig. 1a. This progressive compacting of the structure from the center to the edges is called chirping and it is shown in Fig. 3a.

The decreasing size of fractals towards the edge of the structure improves the matching of the Bloch wave inside the structure with respect to the input and output impedances, and in this way attenuates or eliminates unwanted oscillations of the transmission coefficient in the bandpass region. This effect is even more pronounced if a similar tapering function is applied to the microstrip width [8] as shown in Fig. 3b. In such case, the width of the microstrip line is given by the equation:

$$W_i = W_{max} T(z_i / L) \quad i = 0, 1, \dots, \quad (7)$$

where $W_{max} = 2$ mm. In order to obtain an optimal performance of the frequency response we have introduced a factor K that modulates the tapering of the microstrip width according to the following equation:

$$W_i = K \cdot W_{max} T(z_i / L) \quad i = 0, 1, \dots \quad 0.5 \leq K \leq 2.25 \quad (8)$$

In Fig. 4 we show some examples of the influence of K in KFEBG structures with a Kaiser tapering distribution in the fractal pattern of the ground plane and a Kaiser tapering distribution of the microstrip width.

3 ANALYSIS AND OPTIMIZATION OF CHIRPED AND TAPERED MICROSTRIP KOCH FRACTAL ELECTROMAGNETIC BAND GAP (KFEBG) STRUCTURES

Electromagnetic (EM) simulations and measurements have been carried out in order to compare the performance of the different tapered 1-D KFEBG microstrip structures modified by the proposed K factor. After a thorough investigation of the influence of the K factor, fabrication and testing of the optimal structures was undertaken and the results of the measurements will be presented and compared with the EM simulations. In all simulations and measurements the initial $C=r/a$ factor has been chosen as 0.5. Material with a dielectric constant $\epsilon_r = 10.2$ ($\text{tg}\delta = 0$), substrate thickness $h = 0.635$ mm, and copper thickness $t = 0$ μm has been employed in the simulations as an idealization of the RO3010 material (manufactured by Rogers) that we have used in the experimental measurements ($\text{tg}\delta = 0.0023$ at 10 GHz and copper thickness $t = 17.5$ μm). The different structures have been designed with the purpose to have an operation frequency of 4.2 GHz, so the periodicity of the pattern was chosen as $a = 14.1$ mm ($\lambda_g = 2a$, where λ_g is the guided wavelength in the unperturbed microstrip line) [2-4]. The total number of etched cells (Koch fractal elements) has been set to $N = 9$, as in references [3], [7-10]. At the top plane, the width of the conductor line was $W = 0.594$ mm at the ports, which corresponds to a 50 Ω conventional microstrip line, but the microstrip width changes according to the different tapering distributions modified by the proposed K factor. The prototypes have been fabricated by means of a numerical milling machine. EM simulations have been carried out by a commercial finite element simulator (HFSS), while measurements were done with a vector network analyzer (R&S ZVA67).

In order to establish a criterion for the comparison of the large amount of simulations that we have performed, we have selected four parameters to be extracted from the

simulations: ripple (R_i), return loss (R_L), medium value of S_{11} in the passband ($MVPB$), and band width (B_w) of the passband of the low pass filter. A fifth comparative parameter is obtained from the reduction of size (R_s) of every structure that we have simulated. In the following we define these parameters and present the corresponding results.

The ripple R_i (dB) is defined as the difference between the maximum and minimum value of the transmission coefficient $|S_{21}|$ in the band pass region. A comparison of values of this parameter for each simulated 1-D KFEBG structure versus the K factor is presented in Fig. 5. The lower the value of R_i the better is the performance of the filter. Therefore, a detailed examination of Fig. 5 allows to extract the conclusion that the sharpest tapered distributions in ground plane (Cauchy and Kaiser, Figs. 5a and 5b, respectively) combined with flat tapered distributions (Gauss or rectangular) in microstrip width modified with $K < 1$ are generally the best options for the optimization of this parameter. However, the Cauchy tapering on both sides with factor $K > 1$ (Fig. 5a) is also an interesting option because of the decreasing tendency of the ripple with increasing K factor. We will refer to this structure as the Cauchy double side tapered structure.

The return loss R_L (dB) is the maximum value of the reflection coefficient $|S_{11}|$ in the bandpass region. In the same way as with the previous parameter, the lower the value of the return loss the better is the performance of the filter. Fig. 6 shows the evolution of this parameter as a function of the K factor for each 1-D KFEBG structure. The first conclusion that can be drawn after a detailed examination of Fig. 6 is that the return loss reaches significantly lower values for the Cauchy and Kaiser ground plane distributions compared to the less pronounced Gauss and rectangular distributions. Therefore, if we concentrate our attention in the first two cases (Figs. 6a and 6b), we see that the most interesting features are the minima of the return loss as a function of K . In the case of the Kaiser ground plane distribution (Fig. 6b), the minima are achieved for the rectangular and Gauss microstrip line

modulations. In the case of the Cauchy ground plane distribution (Fig. 6a) there are also interesting minima for these two microstrip line modulations, although shifted to lower K values. However, in this case the most interesting feature is the minimum for the Cauchy double side tapered structure (Cauchy modulation both in the ground plane and in the microstrip line), which appears for a K value of 1.25. As we will see later, this will be one of the structures that we have chosen as optimal.

The next parameter that we have analyzed is the medium value of $|S_{11}|$ in the passband: $MVPB$ (dB). As with the previous two parameters, the lower the value of $MVPB$ the better the performance of the filter is. In Fig. 7 we show the tendency of $MVPB$ as a function of the microstrip line modulation factor K for the four possible types of ground plane fractal distributions that we have studied. If we compare Fig. 7 with Fig. 6, we realize that the values of the $MVPB$ are again significantly lower for the Cauchy and Kaiser ground plane distributions (Figs. 7a and 7b), so we will concentrate our attention in these two cases. The tendencies as a function of the parameter K present minima for each type of microstrip line modulation. As it happened with the return loss in Fig. 6b, the Kaiser ground plane structure seems to work better in combination with the rectangular and Gauss microstrip lines. On the other hand, the structure with the Cauchy ground plane fractal distribution (Fig. 7a) presents interesting minima for both the Kaiser and Cauchy microstrip lines, being the best combination a double side tapered Kaiser (upper plane) – Cauchy (ground plane) structure with $K=1.25$. Something similar happened for the return loss in Fig. 6a, although in that case the best combination was a Cauchy double side tapered structure.

Finally, the last parameter that we have analysed is the bandwidth of the passband of the filter: $BWPB$ (GHz). This parameter is measured for the reflection coefficient S_{11} at 3 dB in the bandpass edge, and it is shown in Fig. 8 as a function of K for all the structures

analysed in this work. All structures show a decreasing tendency of *BWPB* with increasing *K*, so in principle lower *K* values are better for the low-pass performance of the filter.

In order to evaluate the compactness of the filters we define the parameter R_C (%) as the ratio between the sizes of each proposed structure and the largest structure (the one with rectangular tapering). Table 1 shows the values of R_C for the four possible ground plane distributions. R_C depends on the ratio r/a , which is the same for all the structures of our study (and equal to the limiting value of a conventional non-fractal structure: $C=r/a=0.5$). It also depends on the ground plane distribution that determines the distance between fractal cells. The sharpest tapering distribution function provides the most compact structure, which in our case is the Cauchy distribution, as can be seen on Table 1.

As a consequence of the study of the previous parameters, we have selected two structures with double side tapering as the most optimal ones and we have fabricated and tested them. Fig. 9 shows photographs of the upper and lower planes of these structures. The first one (structure 1) has a Kaiser tapered fractal distribution in the ground plane combined with a rectangular tapered distribution in the microstrip line modified with $K= 0.9$. This structure is the optimum one for the parameters associated with the values of the reflection coefficient (S_{11}) in the passband: return loss (R_L) and medium value in the passband (*MVPB*), because it produces the minimum values of these parameters, and also results in very good values for the ripple of S_{21} (R_i). The second structure (structure 2) that we have chosen is a double side tapered Cauchy distribution with $K = 1.25$. This structure is a compromise between the different parameters. It produces the minimum value of return loss in the passband and it is close to the minimum of *MVPB*, although for this later parameter the Kaiser modulation in the microstrip line combined with Cauchy distribution in the ground plane produces a smaller minimum. The reason why we have preferred the Cauchy double side tapered structure is because the values of ripple and bandwidth are slightly better in this case.

The simulated and measured results for the two chosen structures are shown in Fig. 10. A good agreement between simulation and experimental measurements is achieved. These results demonstrate good low pass behaviour with small ripple of S_{21} and low values of S_{11} in the passband. Additionally, these two structures provide the higher degree of compactness compared to the non-tapered fractal ground plane, as can be seen in Table 1 and in the photographs of Fig. 9. In this figure it can be clearly seen that the structure with the Cauchy ground plane fractal distribution provides the higher degree of compactness. Such compactness, together with the low values of ripple, return loss, and *MVBP* make the double side tapered Cauchy structure the option of choice for the best compromise of performance and size reduction.

We have compared the characteristic parameters of both devices with other results of comparable structures that can be found in the recently published literature [3-4], [7-9], [18-19], and also for a classical (non-EBG) low pass filter [20]. Such results are shown in Table 2 for easy comparison. In this table λ_0 is the free-space wavelength at the operation frequency (f_0) of the stopband, and it is used to give the normalized 3-D size of the devices. In the case of the structures of [18], [19] and [20] the sizes given in the table have been calculated for 9 cells. None of the sizes include the microstrip feeding. The parameter 20dB *RBW* is the 20 dB rejection bandwidth for S_{21} , while *SRL* is the maximum stopband rejection level. For each reference, we mention the corresponding figure from where we have obtained the results presented in Table 2. In the case of [8], the results correspond to the solid line of figure 3 in such reference, while for [9] the results correspond to the thick solid line of figure 8 in this later reference. The operational frequency of the stopband f_0 in [18] is determined from the extreme attenuation pole frequencies: $f_0 = \sqrt{3\text{ GHz} \times 9\text{ GHz}} \cong 5.2\text{ GHz}$, while in [20] f_0 corresponds to the maximum *SRL*.

From the analysis of Table 2 we can conclude that the structures optimized in this paper present simultaneously very low values of ripple in the passband, high values of return loss (R_L) of S_{11} in the passband, wide stopband with high rejection level, and a small size. If we consider all of these parameters together, we can observe that our structures present the best compromise between size and performance.

Due to the application of the tapering functions, the condition $r/a \geq 0.5$ necessary to achieve the low pass filtering behaviour of our structures (instead of the Bragg reflector behaviour of conventional EBG structures) can also be achieved with circular shapes. However, in such case the performance of the filters is not as optimal as with the fractal shapes that we have analysed in this paper. In order to compare conventional circular EBG structures with our Koch Fractal EBG devices we have performed simulations of circular structures equivalent to the optimized KFEBG analysed in this paper (devices of Figs. 9a and 9b). The results of this comparison are presented in Table 3 and Table 4. From these tables we can conclude that the fractal devices show better performance than the circular structures for all parameters, although we observe a slight reduction of the bandwidth of the passband in the fractal devices.

If we concentrate on the ripple parameter, whose optimization was the main goal of this study, we can conclude that our structures show a very significant improvement with respect to most conventional EBG structures published in the literature (Table 2) and also with respect to tapered structures with circular patterns (Tables 3 and 4).

4 CONCLUSION

A periodic pattern based on Koch fractals has been applied to 1-D electromagnetic bandgap (EBG) microstrip structures with $r/a = 0.5$, demonstrating a good low pass filter behavior. In order to optimize ripple, return loss, and reduce size, 16 possible combinations of double side

tapered distributions (tapered in ground plane and microstrip width) have been analyzed, and for each of these combinations we have introduced a microstrip width modulation K factor to obtain the best optimal performance in the frequency response. The best structures are the Kaiser tapered distribution in ground plane combined with the rectangular tapered distribution in microstrip width modified with $K = 0.9$, and the double side tapered Cauchy distribution with $K = 1.25$. Simulation results have been successfully corroborated by measurements of the optimal structures.

ACKNOWLEDGEMENTS

This work was supported by Ministerio de Economía y Competitividad of Spain and European Regional Development Funds (TEC2013-47037-C5-5-R).

REFERENCES

- 1 Qian, Y., Radisic, V., Itoh, T.: 'Simulation and experiment of photonic band gap structures for microstrip circuits'. Proc. Asia-Pacific Microwave Conf., Hong Kong, China, Dec. 1997, pp. 585-588
- 2 Radisic, V., Qian, Y., Cocilli, R., Itoh, T.: 'Novel 2-D photonic bandgap structure for microstrip lines', *IEEE Microw. Guided Wave Lett.*, 1998, **8**, (2), pp. 69-71
- 3 Falcone, F., Lopetegui, T., Sorolla, M.: '1-D and 2-D photonic band gap microstrip structures', *Microw. Opt. Technol. Lett.*, 1999, **22**, (6), pp. 411-412
- 4 Lopetegui, T., Laso, M.A., Erro, M.J., Benito, D., Garde, M.J., Falcone, F., Sorolla, M.: 'Novel photonic bandgap microstrip structures using network topology', *Microw. Opt. Technol. Lett.*, 2000, **25**, (1), pp. 33-36
- 5 Fu, Y.Q., Yuan, N.C., Zhang, G.H.: 'A novel fractal microstrip PBG structure', *Microw. Opt. Technol. Lett.*, 2002, **32**, (2), pp. 136-138
- 6 Liu, H.W., Sun, X.W., Li, Z.F.: 'A low pass filter of wide stopband with a novel multilayer fractal photonic band gap structure', *Microw. Opt. Technol. Lett.*, 2004, **40**, (5), pp. 431-432
- 7 Ruiz, J.D., Martínez, F.L., Hinojosa, J.: '1D Koch fractal electromagnetic bandgap microstrip structures with r/a ratios higher than 0.5', *Microw. Opt. Technol. Lett.*, 2011, **53**, (3), pp. 646-649

- 8 Ruiz, J.D., Martínez, F.L., Hinojosa, J.: ‘Novel compact wide-band EBG structure based on tapered 1-D Koch fractal patterns’, *IEEE Antennas Wireless Propag. Lett.*, 2011, **10**, pp. 1104-1107
- 9 Laso, M.A.G., Erro, M.J., Lopetegui, T., Benito, D., Garde, M.J., Sorolla, M.: ‘Optimization of tapered Bragg reflectors in microstrip technology’, *Int. Journal of Infrared and Millimeter Waves*, 2000, **21**, pp. 231-245
- 10 Lopetegui Beregaña, J.M.: ‘Photonic Bandgap Structures in Microstrip Technology’. PhD thesis, Universidad Pública de Navarra, 2002
- 11 Lopetegi, T., Falcone, F., Martínez, B., Gonzalo, R., Sorolla, M.: ‘Improved 2-D photonic bandgap structures in microstrip technology’, *Microw. Opt. Technol. Lett.*, 1999, **22**, (3), pp. 207-211
- 12 Chong, C.K., *et al.*: ‘Bragg reflectors’, *IEEE Trans. Plasma Sci.*, 1992, **20**, (3), pp. 393-402
- 13 Hill, K.O., Metlz, G.: ‘Fiber Bragg grating technology fundamental and overview’, *J. Lighthwave Technol.*, 1997, **15**, (8), pp. 1263-1276
- 14 Harris, F. J.: ‘On the use of windows for harmonic analysis with the discrete Fourier transform’, *Proc. IEEE*, 1978, **66**, (1), pp. 51-83
- 15 Caloz, C., Itoh, T.: ‘Electromagnetic Metamaterials: Transmission Line Theory and Microwave Applications’ (John Wiley & Sons, 2006)
- 16 Eleftheriades, G.V., Balmain, K.G.: ‘Negative-Refraction Metamaterials: Fundamental Principles and Applications’ (John Wiley & Sons, 2005)
- 17 Capolino, F.: ‘Metamaterials handbook: Theory and Phenomena of Metamaterials’ (CRC Press, 2009)

- 18 Ting, S. W., Tam, K. W., Martins, R. P.: 'Miniaturized microstrip lowpass filter with wide stopband using double equilateral U-shaped defected ground structure', *IEEE Microw. Wirel. Comp. Lett.*, 2006, **16**, pp. 240-242
- 19 Zhu, H., Mao, J.: 'Miniaturized tapered EBG structure with wide stopband and flat passband', *IEEE Antennas Wireless Propag. Lett.*, 2012, **11**, pp. 314-317
- 20 Mohra, A.S., Alkanhal, M.A.: 'Small size stepped impedance low pass filters', *Microw. Opt. Technol. Lett.*, 2007, **49**, (10), pp. 2398-2403

Authors' affiliations:

Juan de Dios Ruiz, Félix L. Martínez-Viviente, and Juan Hinojosa

Departamento de Electrónica, Tecnología de Computadoras y Proyectos

Universidad Politécnica de Cartagena

Plaza del Hospital 1

30202 Cartagena, Spain

Corresponding Author: Dr. Felix L. Martinez-Viviente. Email: felix.martinez@upct.es, Fax: +34 968 326 400

Figure captions:

Fig. 1 1-D KFEBG microstrip structure with nine Koch fractal periodic patterns etched in the ground plane

a Uniform distribution without tapering

b Kaiser tapering distribution

Fig. 2 Representation of tapering distributions $T(z/L)$ versus normalized longitudinal position (z/L)

Fig. 3 Kaiser-tapered 1-D KFEBG microstrip structure with chirping and modulated microstrip width

a Ground plane

b Top plane

Fig. 4 Kaiser-tapered 1-D KFEBG microstrip structure with varying period and different values of factor K modifying the microstrip line width

Fig. 5 Comparison of R_i (dB) for each 1-D KFEBG structure versus K factor

a Cauchy tapering distribution in ground plane

b Kaiser tapering distribution in ground plane

c Gauss tapering distribution in ground plane

d Rectangular or uniform tapering distribution in ground plane

Fig. 6 R_L (dB) compared for each 1-D KFEBG structure versus K factor

- a* Cauchy tapering distribution in ground plane
- b* Kaiser tapering distribution in ground plane
- c* Gauss tapering distribution in ground plane
- d* Rectangular or uniform tapering distribution in ground plane

Fig. 7 $MVPB$ (dB) compared for each 1-D KFEBG structure versus K factor

- a* Cauchy tapering distribution in ground plane
- b* Kaiser tapering distribution in ground plane
- c* Gauss tapering distribution in ground plane
- d* Rectangular or uniform tapering distribution in ground plane

Fig. 8 B_w (GHz) compared for each 1-D KFEBG structure versus K factor

- a* Cauchy tapering distribution in ground plane
- b* Kaiser tapering distribution in ground plane
- c* Gauss tapering distribution in ground plane
- d* Rectangular or uniform tapering distribution in ground plane

Fig. 9 Photographs for the most optimal KFEBG structures: Kaiser tapered distribution in ground plane combined with rectangular tapered distribution in microstrip width scaled by $K = 0.9$ (first structure in both photographs), and double side tapered Cauchy distribution with $K = 1.25$ (second structure in both photographs)

- a* Upper plane (microstrip line)
- b* Ground plane

Fig. 10 Simulated and measured results for the most optimal KFEBG structures

a Kaiser tapered distribution in ground plane combined with rectangular tapered distribution in microstrip width scaled by $K = 0.9$

b Cauchy tapered distribution in ground plane combined with Cauchy tapered distribution in microstrip width scaled by $K = 1.25$

Table captions:

Table 1 Factor of compactness R_C (%) for each 1-D KFEBG structure tapered on both sides

Table 2 Comparison between the proposed filters and recently published references

Table 3 Comparison of relevant parameters between the Kaiser/rectangular ($K=0.9$) fractal EBG structure and the equivalent EBG circular structure

Table 4 Comparison of relevant parameters between the Cauchy/Cauchy ($K=1.25$) fractal device and the equivalent EBG circular structure

Figure 1

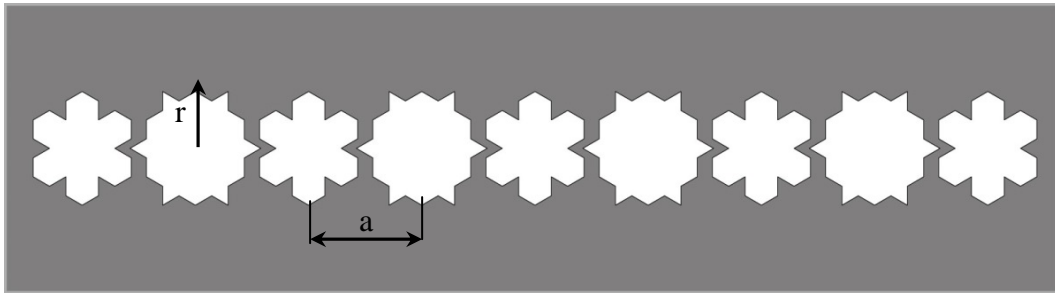
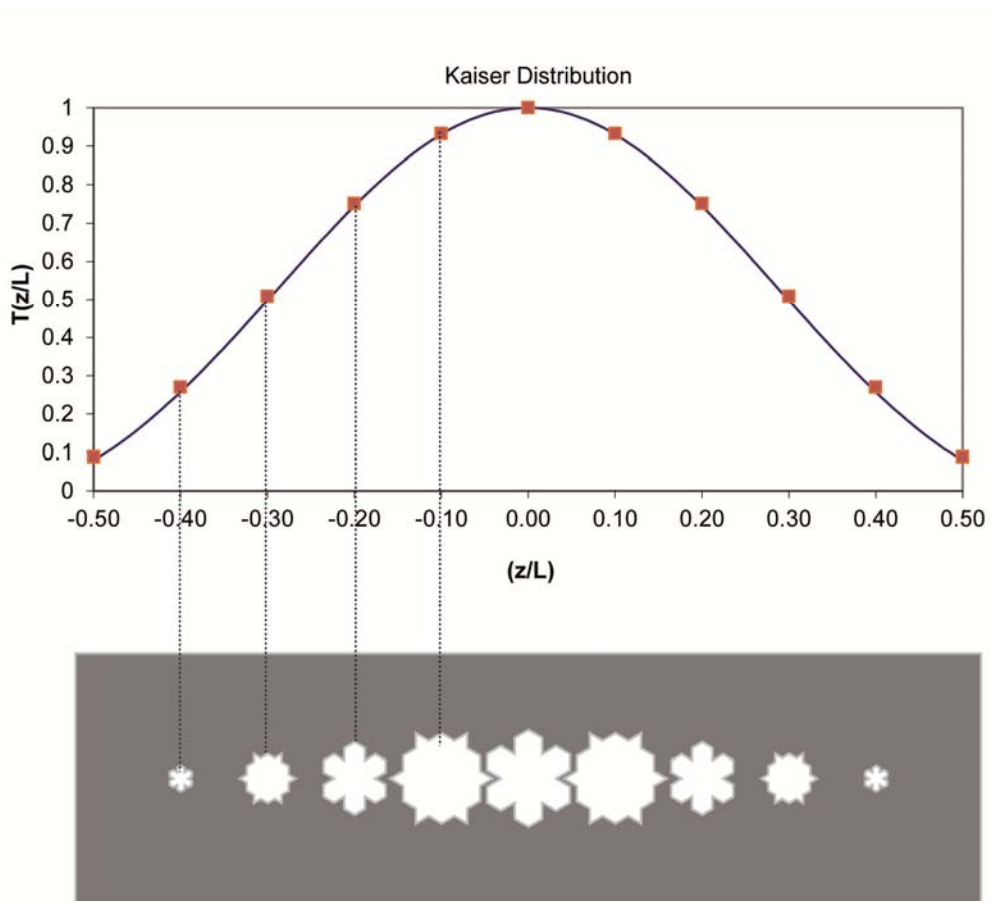
 a  b

Figure 2

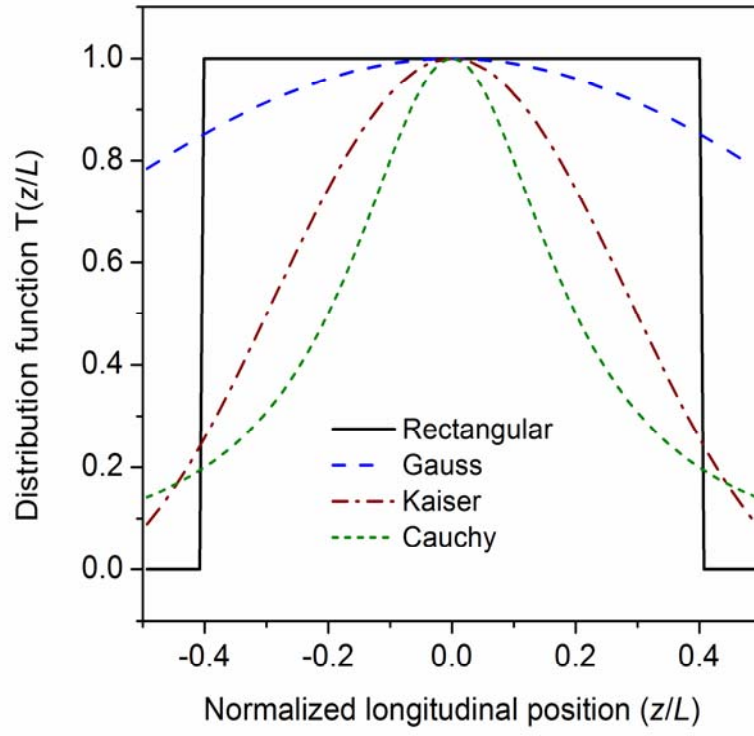
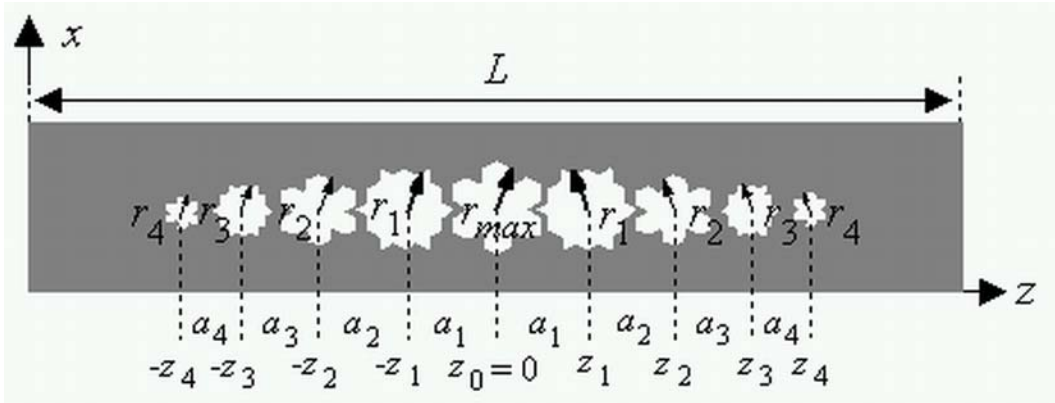
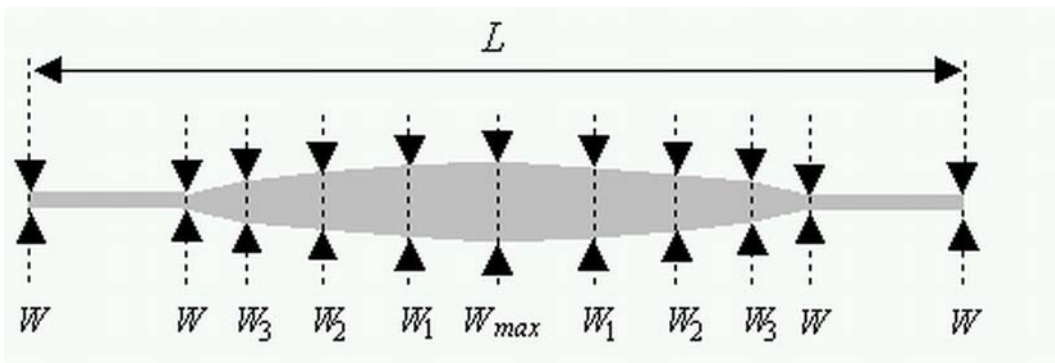


Figure 3



a



b

Figure 4

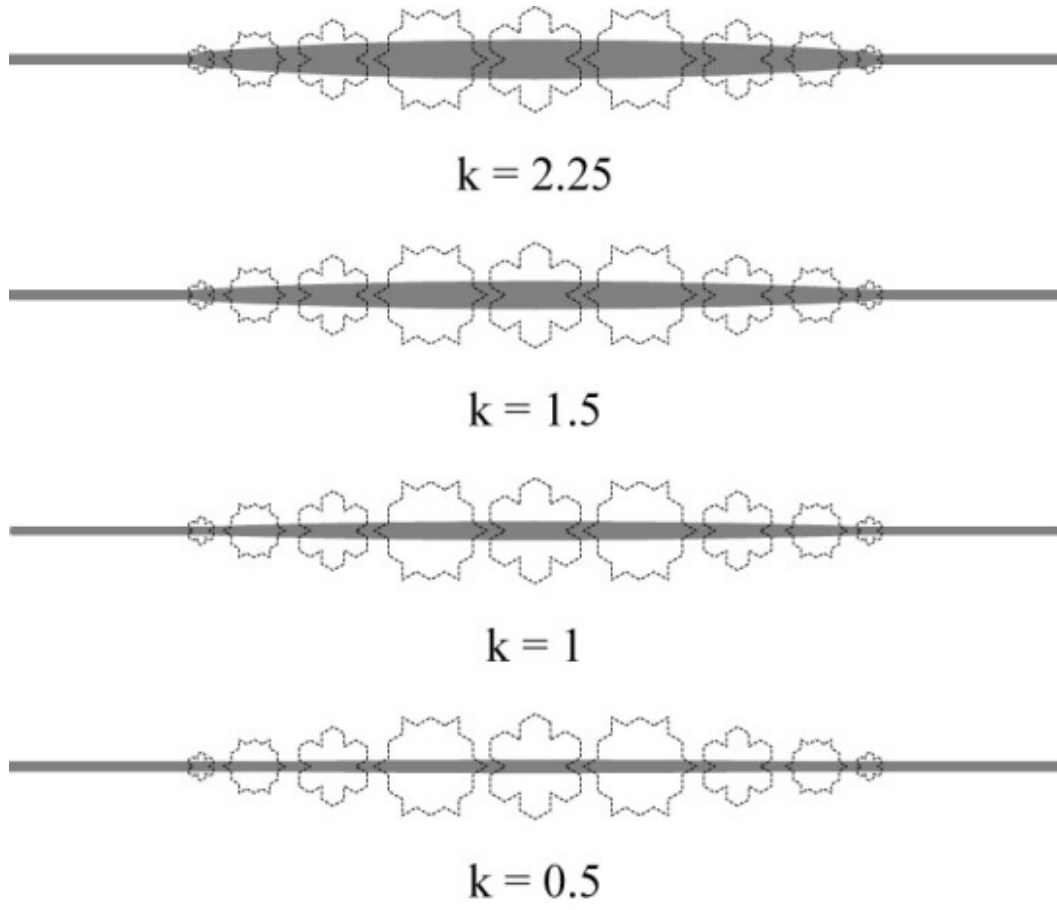


Figure 5

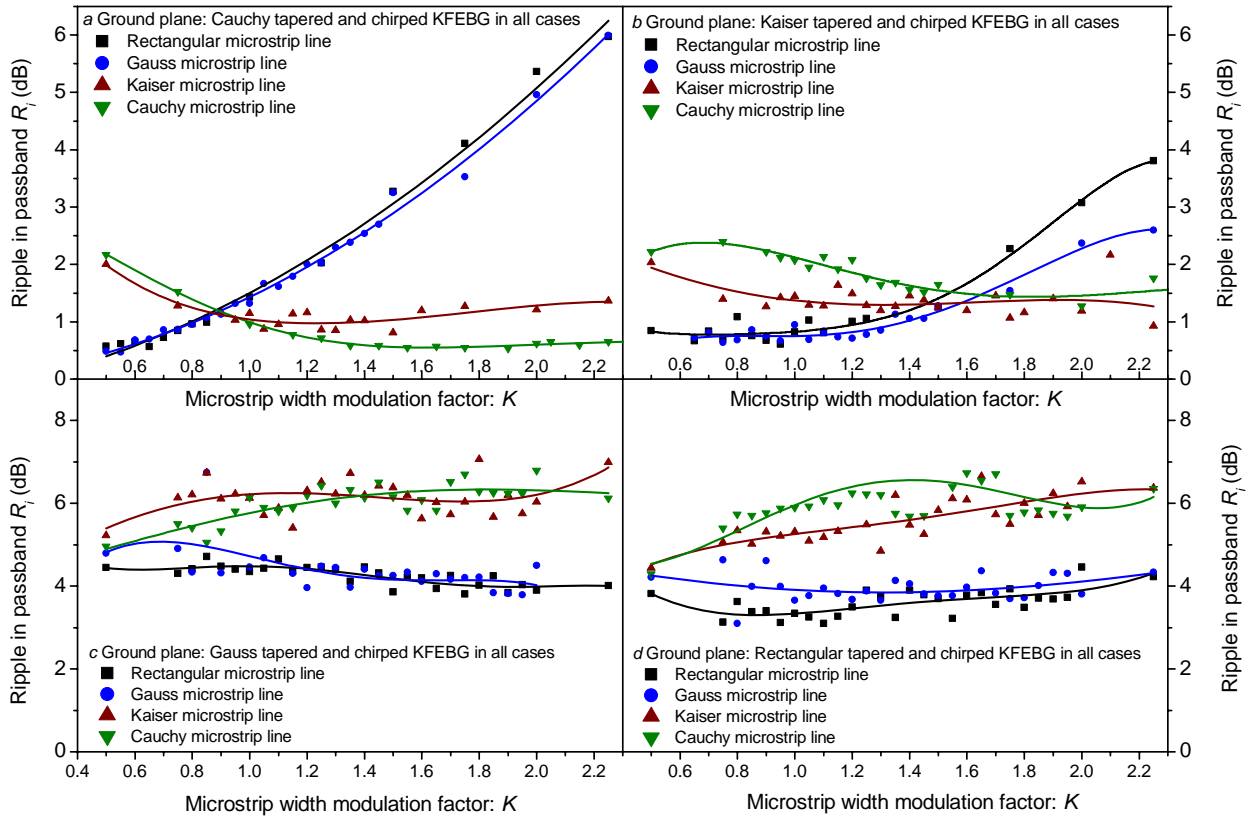


Figure 6

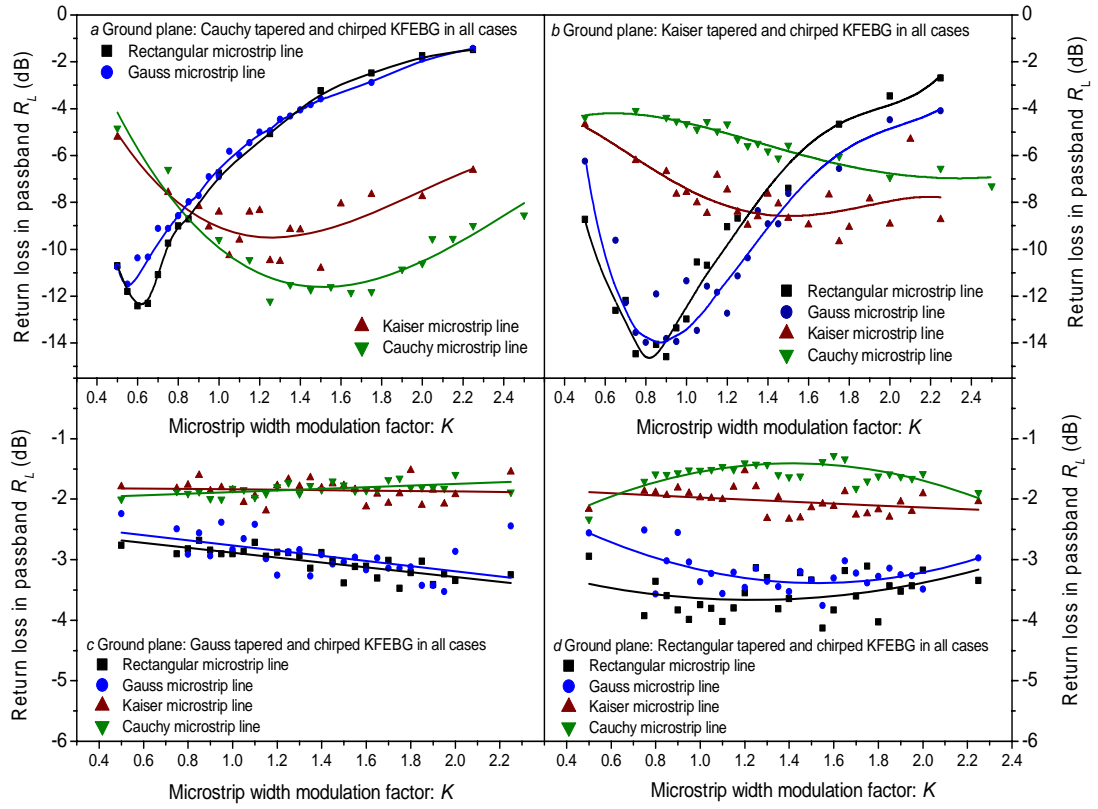


Figure 7

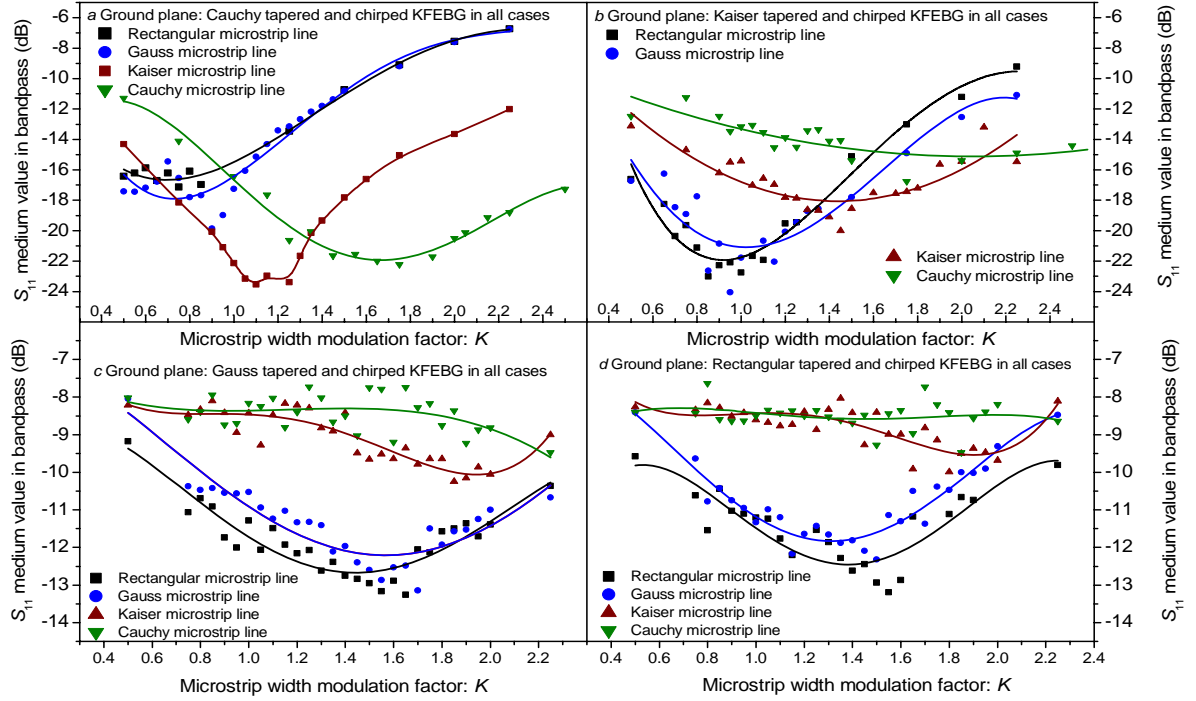


Figure 8

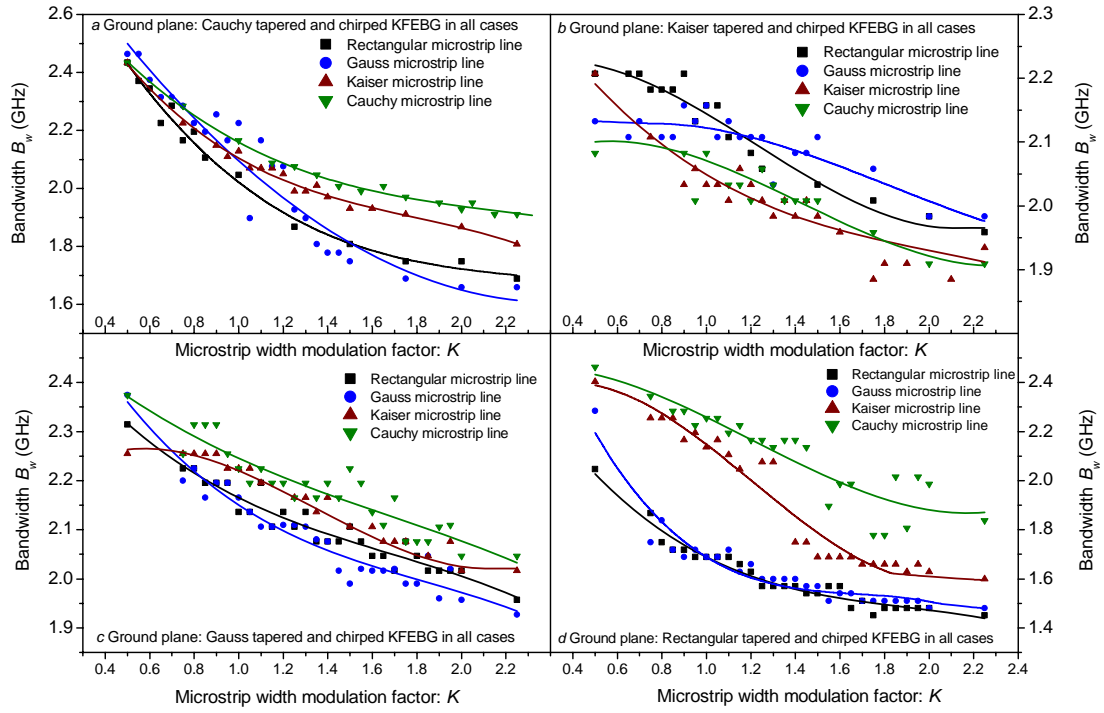
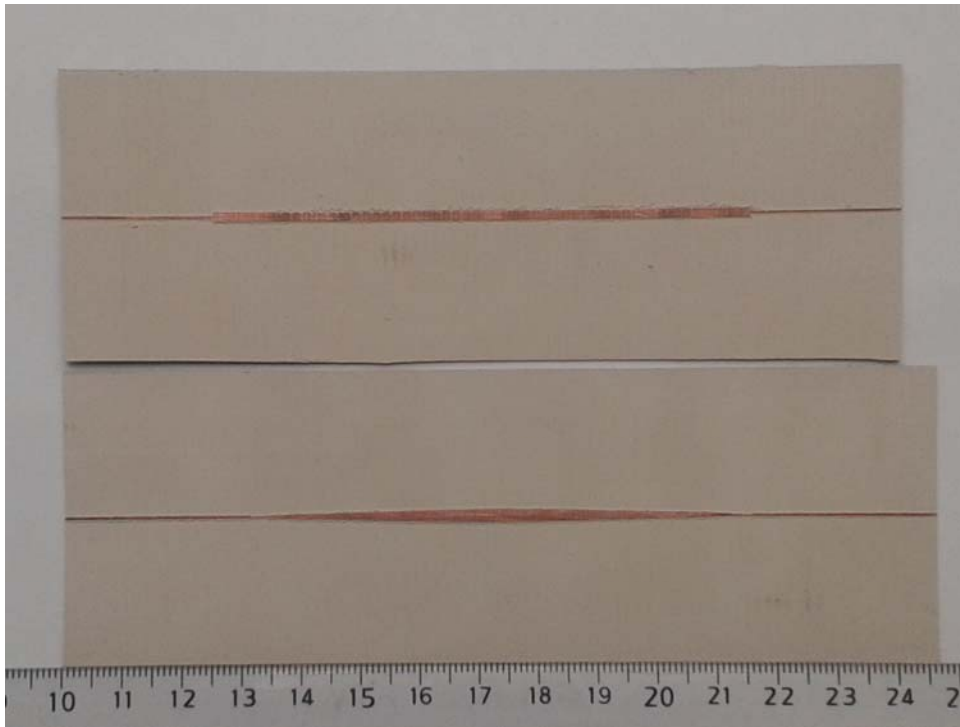
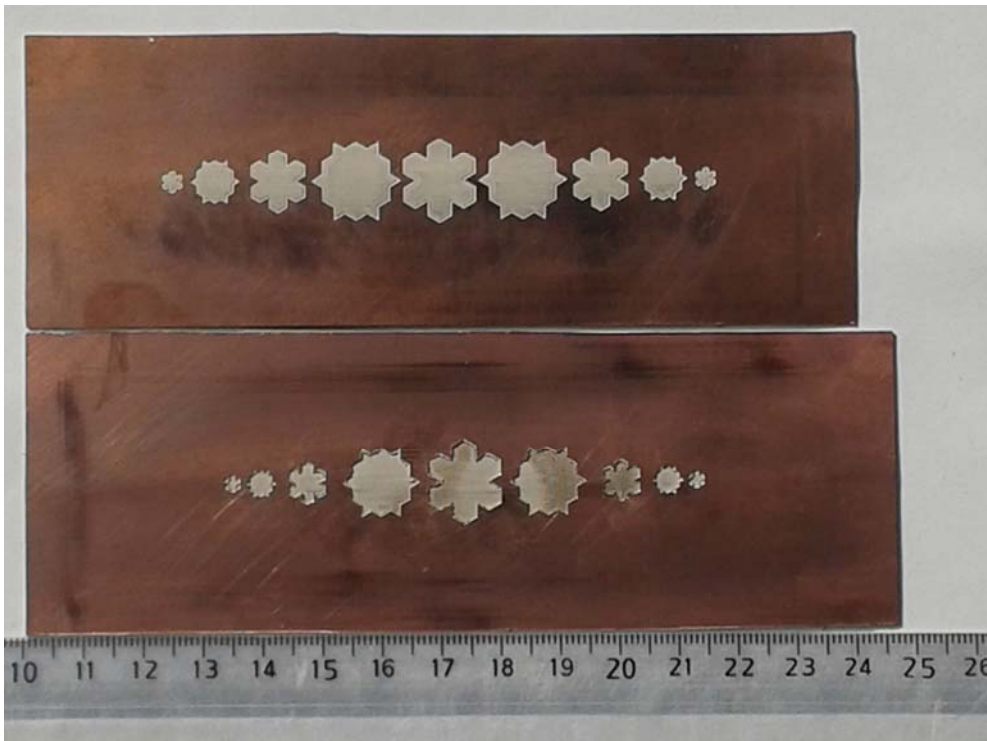


Figure 9



a



b

Figure 10

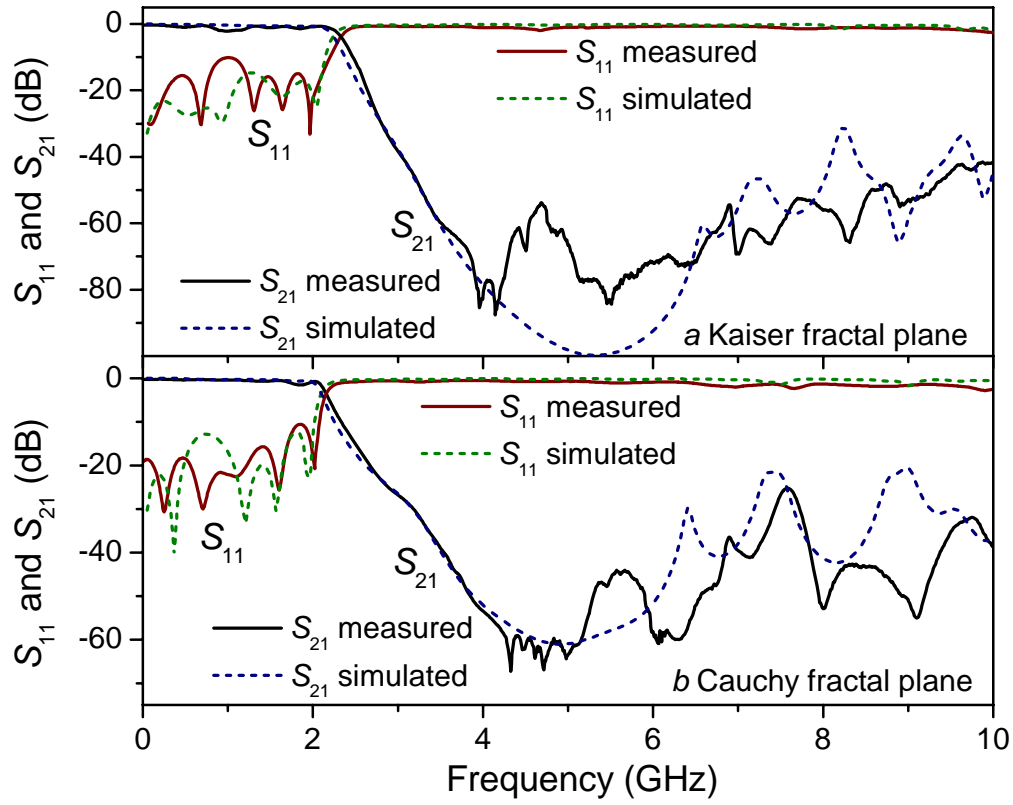


Table 1

	Rectangular	Gauss	Kaiser	Cauchy
R_C	100 %	91 %	73.5 %	63.5 %

Table 2

Ref.	3-D size	f_0 (GHz)	r/a	R_i (dB)	R_L (dB)	20dB RBW (GHz)	SRL
Fig. 10a	$0.19\lambda_0 \times 0.008\lambda_0 \times 1.31\lambda_0$	4.2	0.5	2.2	10.1	> 7.7	80dB@5.2GHz
Fig. 10b	$0.19\lambda_0 \times 0.008\lambda_0 \times 1.07\lambda_0$	4.2	0.5	1.6	10.6	> 7.8	60.9db@4.9GHz z
Fig. 3a [3]	$0.09\lambda_0 \times 0.012\lambda_0 \times 1.60\lambda_0$	3	0.25	-	2	-	-
Fig. 3b [3]	$0.17\lambda_0 \times 0.012\lambda_0 \times 1.68\lambda_0$	3	0.45	-	1	-	-
Fig. 7 [4]	$0.1\lambda_0 \times 0.01\lambda_0 \times 1.79\lambda_0$	2.5	0.25	8	1.4	1.5	60dB@3.2GHz
Fig. 8 [4]	$0.1\lambda_0 \times 0.01\lambda_0 \times 1.79\lambda_0$	2.5	0.25	8	1.4	1.3	49dB@3.2GHz
Fig. 6 [7]	$0.21\lambda_0 \times 0.008\lambda_0 \times 1.79\lambda_0$	4.2	0.55	3.4	-	> 5.4	52dB@4.2GHz
Fig. 6 [8]	$0.21\lambda_0 \times 0.008\lambda_0 \times 1.33\lambda_0$	4.2	0.55	3	4	> 4.7	60db@4.3GHz
Fig. 8 [9]	$0.11\lambda_0 \times 0.016\lambda_0 \times 1.24\lambda_0$	4	0.3	1.3	15.5	0.9	25dB@4.6GHz
Fig. 6 [18]	$0.22\lambda_0 \times 0.026\lambda_0 \times 2.23\lambda_0$	5.2	-	2.3	5	> 7.2	40dB@5.5GHz
Fig. 10 [19]	$0.32\lambda_0 \times 0.018\lambda_0 \times 3.54\lambda_0$	7	0.24	0.8	13	6.5	37.5@8GHz
Fig. 10 [20]	$0.22\lambda_0 \times 0.021\lambda_0 \times 1.28\lambda_0$	4.1	-	1	8	> 2.2 GHz	35@4.1GHz

Table 3

	Ripple R_i (dB) for S_{21} in passband	Bandwidth of pass-band $BWPB$ (GHz)	Medium value of S_{11} in passband $MVPB$ (dB)	Return loss R_L for S_{11} in passband (dB)
Structure 1 Fractal	0.68	2.21	-22.68	-14.59
Structure 1 Circular	0.79	2.53	-20.33	-13.22

Table 4

	Ripple R_i (dB) for S_{21} in passband	Bandwidth of passband BW_{PB} (GHz)	Medium value of S_{11} in passband $MVPB$ (dB)	Return loss R_L for S_{11} in passband (dB)
Structure 2 Fractal	0.72	2.08	-20.62	-12.21
Structure 2 Circular	1.52	2.17	-17.13	-6.56